JACS
JOURNAL OF THE AMERICAN CHEMICAL SOCIETY

ARTICLE

pubs.acs.org/JACS

Role of Water and Carbonates in Photocatalytic Transformation of CO_2 to CH_4 on Titania

Nada M. Dimitrijevic,*[,†,‡] Baiju K. Vijayan,[#] Oleg G. Poluektov,[†] Tijana Rajh,[‡] Kimberly A. Gray,[#] Haiying He,[§] and Peter Zapol[§,†]

[†]Chemical Sciences and Engineering Division, [‡]Center for Nanoscale Materials, and [§]Materials Science Division, Argonne National Laboratory, Argonne, Illinois 60439, United States

[#]Department of Civil & Environmental Engineering, Northwestern University, Evanston, Illinois 60208, United States

Supporting Information

ABSTRACT: Using the electron paramagnetic resonance technique, we have elucidated the multiple roles of water and carbonates in the overall photocatalytic reduction of carbon dioxide to methane over titania nanoparticles. The formation of H atoms (reduction product) and $^{\bullet}OH$ radicals (oxidation product) from water, and CO_3^{-} radical anions (oxidation product) from carbonates, was detected in CO_2-saturated titania aqueous dispersion under UV illumination. Additionally, methoxyl, $^{\bullet}OCH_3$, and methyl, $^{\bullet}CH_3$, radicals were identified as reaction intermediates. The two-electron, one-proton reaction proposed as an initial step in the reduction of CO_2 on the surface of TiO_2 is supported by the results of first-principles calculations.

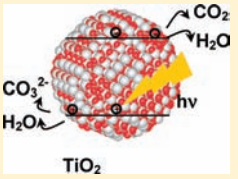

INTRODUCTION

Photocatalytic reduction of CO_2 to formaldehyde, formic acid, methanol, and methane as main products over semiconductor particles was demonstrated three decades ago.[1] Since then, there has been an effort to design an efficient and selective photocatalytic system for the reduction of CO_2 in water that can work without any loss of the light energy through chemical storage.[2−4] The focus has been on TiO_2, an efficient photocatalyst for environmental applications, because it is highly stable, nontoxic, and cheap and absorbs part of the solar spectrum. The use of titania and water (without sacrificial hole scavengers) ultimately provides a "green chemistry" approach to the transformation of CO_2 to fuel. However, the photoefficiency of CO_2 reduction to methane over titania is very low, <0.1%, using only water as an electron donor. The majority of research is aimed at improving photocatalytic efficiency and/or harvesting visible light. The improved efficiency of CO_2 reduction was demonstrated for the synthesized novel titania-based nanomaterials having specific surface structures,[5,6] for coupling titania to dyes,[7,8] enzymes,[9] metallic catalysts,[10,11] or quantum dots.[12] Still, a better understanding of processes that occur on the surface of TiO_2 during carbon dioxide reduction, including adsorption/desorption of CO_2 and intermediate products, as well as the role of adsorbed water is needed in order to elucidate the reaction mechanism which, in synergy with targeted synthesis, can improve overall efficiency.

The reduction of CO_2 to methane is a multistep process, generally presented by the set of eqs 1−4.[13−16] In aqueous dispersions/solutions, electrons are provided by photoexcitation of TiO_2 (conduction band electrons), while water acts as both a proton donor (eqs 1−4) and an electron donor (eqs 5−7). All potentials are presented in reference to NHE at pH 7.

$$CO_2 + 2H^+ + 2e_{CB}^- \rightarrow HCOOH \quad E^\circ = -0.61\ V \tag{1}$$

$$HCOOH + 2H^+ + 2e_{CB}^- \rightarrow HCHO + H_2O \quad E^\circ = -0.48\ V \tag{2}$$

$$HCOH + 2H^+ + 2e_{CB}^- \rightarrow CH_3OH \quad E^\circ = -0.38\ V \tag{3}$$

$$CH_3OH + 2H^+ + 2e_{CB}^- \rightarrow CH_4 + H_2O \quad E^\circ = -0.24\ V \tag{4}$$

$$H_2O + h_{VB}^+ \rightarrow OH + H^+ \quad E^\circ = +2.32\ V \tag{5}$$

$$2H_2O + 2h_{VB}^+ \rightarrow H_2O_2 + 2H^+ \quad E^\circ = +1.35\ V \tag{6}$$

$$2H_2O + 4h_{VB}^+ \rightarrow O_2 + 4H^+ \quad E^\circ = +0.82\ V \tag{7}$$

Although conduction band electrons of TiO_2, $E_{CB} = -0.50$ V at pH 7,[17] are sufficiently energetic to drive CO_2 reduction to methane, $E^\circ(CO_2/CH_4) = -0.24$ V, the detailed mechanism is not well understood, and it is proposed to involve shared intermediates and multiple reaction pathways starting with the formation of CO_2^- radical anion bound to the oxide surface.[18] To our knowledge, there is very little experimental data on the reaction intermediates. The formation of surface-adsorbed

Received: September 29, 2010
Published: February 24, 2011

CO_2^- on MgO in the absence of water and in the presence of excess electrons has been confirmed by electron paramagnetic resonance (EPR),[19−21] while formation of CO_2^- at the surface of TiO_2 under UV illumination was detected by infrared (IR) spectroscopy.[22] Carbonate, bicarbonate, formic acid, formaldehyde, and methoxy have been observed on the oxide surfaces during CO_2 reduction.[11,20]

In general, a low yield of methane production over titania is attributed to two major factors: (i) the strong oxidizing power of valence band holes (E_{VB} = +2.70 V vs NHE at pH 7) that can result in the reaction of holes (or OH radicals) with intermediate molecular products (formate, formaldehyde, methanol), and (ii) the thermodynamically unfavorable one-electron reduction of CO_2, based on a very negative redox potential for this process in an aqueous homogeneous system, $E^\circ(CO_{2\,aq}/CO_2^-{}_{aq})$ = −1.9 V vs NHE. However, the presence of proton donors together with the binding of CO_2 to the oxide surface could diminish redox potential by almost an order of magnitude.[23,24] Anpo and coworkers probed the properties of highly reactive titania-based oxide materials as related to CO_2 reduction and showed that the product yields depend strongly on the coordination of surface Ti atoms, the H_2O:CO_2 ratio (maximum for 5:1), and the reaction temperature.[5] They demonstrated that the yield of methane production increases with the concentration of undercoordinated Ti at the surface.[5] Carbon dioxide adsorbs preferentially on undercoordinated Ti surface sites, both five-[25] and four-coordinated.[5] The proximity/binding of CO_2 to the surface not only affects its redox properties but competes with the recombination of charges, a thermodynamically favored process.

In contrast to CO_2, water dissociates on the surface of TiO_2; i.e., water oxygen forms a dative bond with a surface Ti, whereas the hydrogens form two weak H-bonds with bridging oxygens,[26−28] giving rise to the formation of both terminal and bridging OH groups at the surface. Molecular H_2O is further bound to these OH surface groups, and more than three layers constitute a bulk water.[29] This strong binding/dissociation translates to the lowering of the barrier for a one-electron-transfer process. Furthermore, water solvates CO_2, and at room temperature 0.2−1% of solvated/dissolved CO_2 is in a form of carbonic acid, eq 8. Interaction of carbonic acid with an OH-functionalized surface could lead to dehydration and binding of bicarbonate, or bicarbonate ions can be present in TiO_2/water double layer, in both cases participating in a photocatalytic process.

$$K_{eq} = \frac{[H_2CO_3]}{[CO_2]_{aq}} \approx 1.7 \times 10^{-3} \qquad (8)$$

In this paper we address the role of water and dissolved CO_2 in the form of carbonates/bicarbonates in the overall mechanism/efficiency of CO_2 reduction on titania, in the absence of sacrificial hole scavengers, applying EPR spectroscopy. EPR techniques enable studies of photogenerated charges localized on titania and charge-transfer processes leading to formation of paramagnetic radicals directly or indirectly via a spin-trap method. As a photocatalyst we have chosen Degussa P25 Aeroxide to avoid discrepancies in materials synthesized in different laboratories, and because it is widely used as a reference material for demonstrating the efficiency of various photocatalysts. In this work we compare data for partially hydrated and fully hydrated titania surfaces in the absence and in the presence of adsorbed CO_2.

EXPERIMENTAL SECTION

Materials. Sodium carbonate (Aldrich), acetonitrile (Sigma), and the spin trap 5,5-dimethyl-1-pyrrolyne *N*-oxide (DMPO, Sigma) were all analytical grade and used as received, without further purification. Research-grade carbon dioxide, 99.999% (Airgas), was passed consecutively through two hydrocarbon traps (Supelco) to remove even a trace amount of impurities. Powdered TiO_2 (Degussa P25 Aeroxide) was used as received; no heat treatment was used to remove bound water. Milli-Q water was used immediately upon production to reduce dissolution of carbon dioxide from air. TiO_2 was left in D_2O (Cambridge Isotope Laboratories) for 3 months in order to exchange bound water. Samples were degassed at 77 K using a 10^{-5} bar vacuum system, and a controlled amount of CO_2 gas (in the range 300−700 mbar) was introduced into suprasil EPR tubes (Wilmad LabGlass).

Instrumentation. X-band continuous-wave EPR experiments were conducted on a Bruker Elexsys E580 spectrometer equipped with an Oxford CF935 helium flow cryostat with an ITC-5025 temperature controller. EPR spectra of photogenerated charges were recorded at cryogenic temperatures, from 4.5 to 77 K, while measurements using DMPO spin trap were performed at room temperature. The *g* factors were calibrated for homogeneity and accuracy by comparison to a coal standard, $g = 2.00285 \pm 0.00005$. The weak pitch reference sample, in combination with a known concentration of TEMPO radicals (2,2,6,6-tetramethylpiperidine-1-oxyl, Aldrich), was applied for quantitative analysis. Double integration of the EPR spectra was carried out using the Bruker data analysis package after baseline correction. Samples were excited either with 355 nm photons from Nd:YAG laser (power 9 mJ) or by using a 300 W Xe lamp (ILC) with a photon flux of 1 mmol m^{-2} s^{-1}.

An HP 5890 gas chromatograph equipped with a flame ionization detector (GC-FID) was used to monitor photocatalytic production of methane. Production of CH_4 was measured in a closed reactor at room temperature containing 10 mg of TiO_2 (P25) and CO_2/water vapor (atmospheric pressure) under continuous illumination with 365 nm photons from a mercury vapor UV lamp (100 W), energy density of 110 W/m^2. The sample holder was a circular pot with a diameter of 1.8 cm (total area for irradiation). The details of catalytic test activity are presented elsewhere.[30]

Computational Methods. A periodic slab model was used to calculate the interactions on the surface. Our model system represents an anatase (101) surface, which is the most abundant surface in anatase featuring two types of under coordinated atoms: five-fold Ti atoms and two-fold O atoms. A 2×1 supercell along the [010] and [101] directions consisting of six TiO_2 trilayers with four Ti atoms per layer was used. Atoms in the bottom trilayer were fixed to their bulk positions. A vacuum layer of about 11 Å was placed between slabs along the *z* direction. Calculations were done using PBE exchange correlation functional,[31] plane wave basis sets, and PAW potentials as implemented in the VASP program.[32] The PBE functional has previously proved to reproduce experimental results of the structural and energetic properties of TiO_2 bulk and surfaces.[33] A Monkhorst−Pack grid of 2×2×1 was used to sample the first Brillouin zone. The total energy is converged to 10^{-5} eV, and the force on each atom is converged to 0.03 eV/Å. A hydrogen atom is introduced on the surface-bridging two-fold O atom to become a proton with a formal charge state of +1. The electron from this H redistributes over Ti atoms to populate the bottom of the TiO_2 conduction band within self-consistent calculations mimicking a photoexcited electron, while the proton mimics a localized hole in terms of its Coulomb potential.[34] Charge distribution (see Supporting Information) is analyzed using Bader charge analysis.[35] Transition states along the reaction pathways were located with the Climbing Image Nudged Elastic Band method.[36]

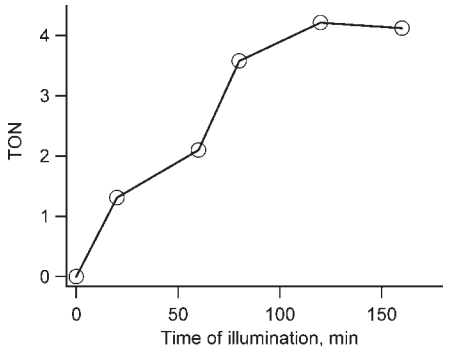

Figure 1. Production of CH_4 measured in a closed reactor containing 10 mg of TiO_2 (P25) and CO_2/water vapor (atmospheric pressure) under continuous illumination with 365 nm photons. For calculating TON, the values of 10^{15} active sites/m^2 and surface area of 55 m^2/g for P25 were taken into account.

RESULTS AND DISCUSSION

The photocatalytic reduction of CO_2 to CH_4 was demonstrated for TiO_2 P25, a mixed-phase anatase/rutile titania. Figure 1 presents the turnover number (TON), expressed as a number of CH_4 molecules formed per number of surface active sites (typically $10^{10}-10^{12}$ per cm^2),[37] under bandgap excitation of TiO_2 at room temperature in a system containing only carbon dioxide and water vapor at atmospheric pressure. The quantum yield of the order of 10^{-3} (Supporting Information) is comparable to the ones previously reported for various titania nanocomposites, including pure anatse nanoparticles, mixed-phase or nitrogen-doped titania, and TiO_2 in the presence of metallic cocatalysts.[5]

EPR spectroscopy has been widely used to examine paramagnetic species formed upon bandgap excitation of TiO_2, including P25.[38] Excitation of nanocrystalline TiO_2 with photon energies larger than its bandgap results in the femtosecond formation of conduction band electrons and valence band holes. Once produced, the charge carriers become trapped into lower energy states (shallow and deep traps), accompanied by their recombination. The strategy of using temperatures below 80 K in EPR measurements allows for the detection of localized charges in titania, since the rate of electron−hole recombination is reduced at these temperatures.[39] It was demonstrated by EPR that, when TiO_2 is illuminated at temperatures <10 K, photogenerated electrons localize in the interior of nanoparticles, while holes, due to their higher mobility,[40] localize on surface oxygen, forming $(Ti^{3+})_{latt}$ and $(Ti^{4+}O^{\bullet-})_{surf}$ paramagnetic species, respectively.[39,41] Due to their strong oxidation power, surface-trapped holes react with adsorbed molecules even at these extremely low temperatures.[42] On the other hand, for electrons to react with adsorbed molecules, an increase in temperature is required, usually >30 K, because it allows for detrapping of electrons from lattice to conduction band and their further migration to the surface (the activation energy for detrapping from lattice shallow traps is ~20 meV).[43] Once photogenerated electrons reach the surface of TiO_2, they can react with adsorbed molecules or localize on surface trapping sites (Scheme 1). The exception arises when electron-accepting molecules make strong complex with surface titanium ions, which allows molecules to compete for conduction band electrons with their thermalization/localization on lattice trapping sites. This was shown previously for pyrroloquinoline quinone (PQQ), which forms

Scheme 1. Salient Presentation of the Energetics of Photogenerated Charges, As Observed by EPR under Illumination of TiO_2 at Different Temperatures

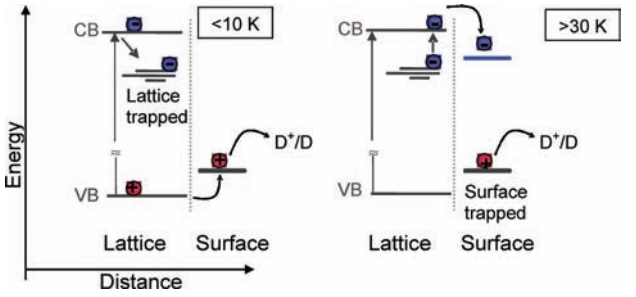

a strong tridentate complex with Ti^{4+} ions on the surface of anatase nanoparticles, resulting in a one-electron reduction of PQQ to semiquinone, to some extent even at extremely low temperatures, below 30 K.[43] Thus, our strategy was to illuminate a reaction mixture of $TiO_2/CO_2/H_2O$ at a higher temperature, 77 K, in order to increase the yield of reducing reactions, and to record EPR spectra at 4.5 K, in order to increase the sensitivity of the measurements.

The EPR spectrum recorded in the dark at 4.5 K after 1 h illumination of TiO_2 in the presence of CO_2 and H_2O at 77 K is presented in Figure 2. The spectrum consists of multiple paramagnetic species having different g-tensor values and hyperfine splittings. The EPR signals with $g_\perp = 1.991$ and $g_\perp = 1.975$ are attributed to electrons trapped in the lattice of anatase and rutile, $(Ti^{3+})_{latt}$, respectively.[38] The signal from holes localized on the surface of titania, $(Ti^{4+}O^{\bullet-})_{surf}$, is also denoted in Figure 2. The two-line signal with 50.8 mT hyperfine splitting corresponds to H atoms,[44] while $^{\bullet}CH_3$ radicals are identified by a four-line spectrum with intensity ratios of 1:3:3:1, having g-tensor of 2.002 and hyperfine splitting constant $a_H = 2.3$ mT.[45] Similar spectra were observed previously upon illumination of anatase-type TiO_2.[5] These results suggest that photogenerated electrons react not only with CO_2 but also with protons from H_2O bound/dissociated on the TiO_2 surface. Therefore, in the overall photocatalytic process of CO_2 reduction, *water acts as an electron acceptor*. Competitive formation of H atoms with transfer of electrons to carbon dioxide was previously suggested by Anpo[5] and Wu.[11] When H_2O was exchaned with D_2O, no signals from H atoms or $^{\bullet}CH_3$ radicals were observed upon illumination under the same conditions; instead, a seven-line spectrum with hyperfine splitting of 0.36 mT, corresponding to $^{\bullet}CD_3$ radicals, was detected (Figure 3). Due to the low sensitivity of EPR signals, spectra of D and $^{\bullet}CD_3$ radicals were greatly masked by intense signals from holes and electrons on titania.

Methyl radicals, the last intermediate species in the overall reduction process, were the only radicals observed in the EPR spectra. Their concentration increases with a decrease in H_2O:CO_2 molar ratio and with the time of illumination. The yield of $^{\bullet}CH_3$ radicals is directly correlated to the decrease in the concentration of electrons localized on TiO_2 (Supporting Information).

Multiple Roles of Water. In order to further reveal the role of water in a complex photocatalytic process, we have examined charge separation in TiO_2 having partially and fully hydrated surfaces in the absence of CO_2. A "dry" powder TiO_2 P25, as was used in these studies, is partially hydrated having 1.7−4.5 OH groups/nm^2,[46] while dispersing P25 in water results in fully

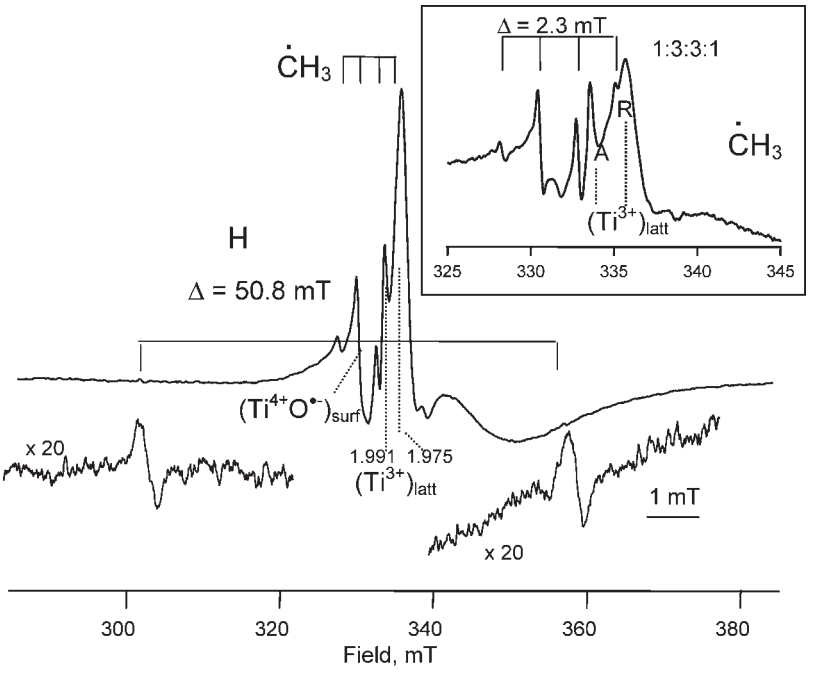

Figure 2. EPR spectrum recorded at 4.5 K after 1 h of illumination at 77 K. Light source, 300-W Xe lamp; sample, 50 mg of TiO_2, 2.8 mmol of H_2O, and 2.8 mmol of CO_2. Instrument conditions: power, 2.0 mW; modulation amplitude, 0.5 mT. For both the inset and detailed detection of H atom signals, power was reduced to 0.2 mW and modulation amplitude to 0.2 mT.

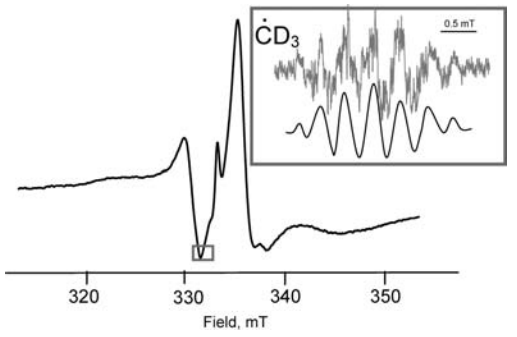

Figure 3. EPR spectrum recorded at 4.5 K after 1 h of illumination at 77 K of 50 mg of TiO_2, 2.8 mmol of D_2O, and 2.8 mmol of CO_2. Instrument conditions and light source as in Figure 2. Inset: experimental EPR spectrum after baseline correction, recorded at 20 K, 6 mW power, and 0.1 mT modulation amplitude, and simulated spectrum of CD_3 radical.

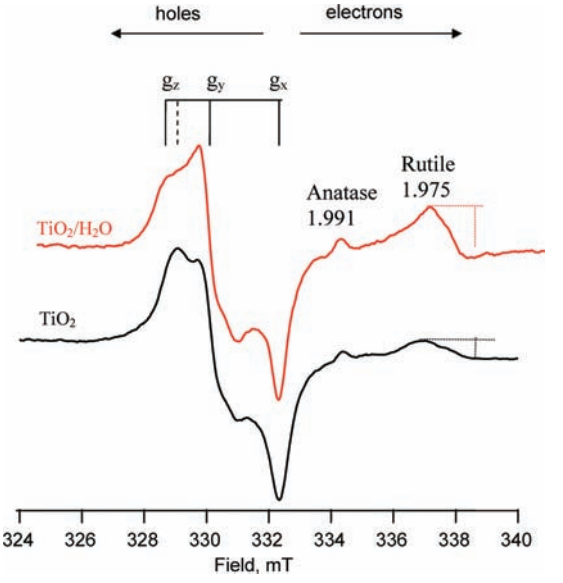

Figure 4. EPR spectra recorded under illumination at 4.5 K of degassed "dry" TiO_2 (black line) and aqueous TiO_2 (red line). Power, 0.2 mW; modulation amplitude, 0.5 mT; light source, 355 nm photons from a Nd:YAG laser (power 9 mJ).

hydrated surfaces. When a vacuum-degassed aqueous dispersion of TiO_2 was illuminated at 4.5 K, the signals from lattice-trapped electrons in both anatase ($g_\perp = 1.991$) and rutile ($g_\perp = 1.975$) and surface-trapped holes were observed (Figure 4). The oxygen-centered radical, due to the trapping of holes on the surface of titania, is characterized by $g_x = 2.002$, $g_y = 2.017$, and $g_z = 2.026$ in the aqueous dispersion and can be assigned according to the previous studies to a $(Ti^{4+}O^{\bullet-})_{surf}$ paramagnetic species.[39,41,47] At the same time, for partially hydrated "dry" TiO_2, a slight shift ($g_z = 2.023$) and an increase in intensity of the g_z component can be observed. The differences suggest that, for partially hydrated surfaces, holes localize on lattice oxygen atoms located in the subsurface layer with a structure of $[Ti^{4+}O^{\bullet-}Ti^{4+}OH^-]$,[41] as the magnitude of the g_z component is largely controlled by the local electric field gradient.

Another possibility to explain the differences between EPR spectra of partially and fully hydrated surfaces is the contribution of OH radicals formed upon excitation of TiO_2 in an aqueous dispersion. The formation of OH radicals from *water acting as an electron donor* is well established (eq 5),[48] and an EPR spin-trap technique is commonly used for their detection (see further text).[49] If any, the contribution of OH radicals to the overall EPR spectrum presented in Figure 4 is extremely low, as no changes in the values or intensities of g_x and g_y components could be observed. It was demonstrated that OH radicals on the surface of metal oxides not only lead to the broadening and decrease in intensity

dx.doi.org/10.1021/ja108791u |*J. Am. Chem. Soc.* 2011, 133, 3964–3971

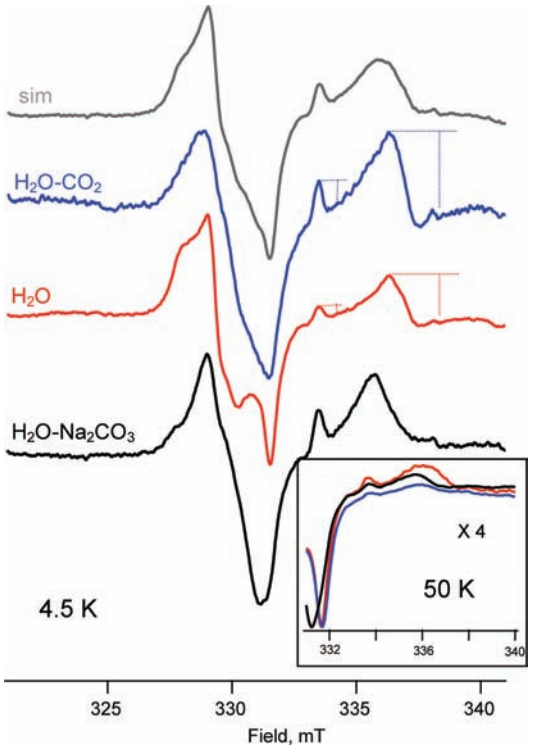

Figure 5. EPR spectra recorded under illumination at 4.5 K of 10 mg of TiO_2 in the presence of (a) 5 mmol of CO_2 and 2 mmol of H_2O (blue line), (b) 2 mmol of H_2O (red line), and (c) 0.5 M aqueous Na_2CO_3 (black line). The simulated spectrum is presented as a gray line. Power, 0.2 mW; modulation amplitude, 0.5 mT. Inset: part of the EPR spectra that corresponds to photogenerated electrons of the same samples illuminated and measured at 50 K (power, 2.0 mW). The light source was 355 nm photons from a Nd:YAG laser (power, 9 mJ).

of the g_z component compared to O^- radicals but also exhibit different values of all three *g*-components.[50]

More importantly, the presence of bulk water and/or a fully hydrated surface enables better charge separation. We have found that the number of spins increases from 0.8×10^{15} spins/cm^3 for "dry" TiO_2 to 1.0×10^{15} spins/cm^3 for aqueous TiO_2 dispersion. As can be seen from Figure 4, the intensities of signals associated with trapped electrons in rutile and anatase are noticeably higher for fully hydrated titania. For better visualization, the signals corresponding to holes/oxidation products are normalized for different spectra presented in Figures 4 and 5, and lines are drawn to indicate relative intensities of photogenerated electrons. As the EPR spectra were recorded under illumination, the intensities of the signals correspond to the steady-state concentrations of products, in our case ruled by the formation and recombination of electrons and holes and products of their subsequent reactions.

In the presence of bulk water, *charges are stabilized* either due to the dipolar interaction with water or due to the band bending at the TiO_2/water interface, which results in suppressed charge recombination.

Role of Carbonates. When CO_2 was added to an aqueous TiO_2 dispersion, further changes in the EPR spectra of photogenerated charges were observed upon illumination at 4.5 K (Figure 5). First, an even higher concentration of spins was observed compared to that in pure water, revealing better charge separation, and second, the line shape and *g*-tensor values of signals associated with holes/oxidation products differ from those in water. We propose that, for dissolved CO_2 in aqueous TiO_2 dispersions, where some of the CO_2 is transformed into carbonic acid, the observed changes in the EPR spectrum are due to the contribution of a signal associated with the formation of CO_3^- anions. The *carbonate/bicarbonate ions act as hole scavengers*, as shown in eq 9a.

$$h_{VB}^+ + CO_3^{2-} \rightarrow CO_3^- \quad (9a)$$

$$h_{VB}^+ + HCO_3^- \rightarrow CO_3^- + H^+ \quad (9b)$$

As a proof of the role of carbonates, the spectrum of illuminated, degassed, aqueous 0.5 M Na_2CO_3/TiO_2 is presented in Figure 5, showing formation of CO_3^- radical anions. The principal *g*-tensor values, $g_x = 2.006$, $g_y = 2.012$, and $g_z = 2.019$, observed for the Na_2CO_3/TiO_2 reaction mixture are in agreement with literature values for orthorhombic CO_3^- radical anions in proximity of K^+, Na^+, or Ca^{2+} cations[51] and suggest binding/adsorption of CO_3^- to $Ti^{4+/3+}$ ions. The formation of CO_3^- results in suppressed charge recombination, seen as an increased intensity of signals associated with electrons localized in anatase and rutile lattices, as charges become spatially separated.

The experimental EPR spectrum of $TiO_2/H_2O/CO_2$ is overlapped and superimposed with spectra corresponding to holes on titania and to CO_3^- radical anions. The simulated spectrum presented in Figure 5 is a sum of the spectra of these two paramagnetic species (with 60% contribution from $(Ti^{4+}O^{\bullet-})_{surf}$ and 40% from CO_3^- radicals).

When temperature was increased to 50 K, lower yields of lattice- and surface-trapped electrons for the $TiO_2/H_2O/CO_2$ reaction mixture as compared with TiO_2/H_2O were observed (Figure 5, inset). When the temperature is increased, the contribution of reaction of photogenerated electrons with adsorbed CO_2 molecules on titania increases and competes with the charge recombination process, as discussed previously and presented in Scheme 1. A slight decrease in the concentration of photogenerated electrons was also observed for a 0.5 M Na_2CO_3/TiO_2 mixture as compared to TiO_2/H_2O; however, the mechanism is not clear. Although reduction of HCO_3^- to formate over Pd/TiO_2 in the presence of the sacrificial hole scavenger oxalate was proposed previously,[52] we cannot rule out a contribution of the reaction of adsorbed CO_3^- anions with photogenerated electrons at elevated temperatures under steady-state conditions, CO_3^- being a strong, one-electron oxidation agent.

EPR Spin Trapping. To further examine the role of water and carbonates, and to identify possible radicals formed upon illumination, the spin-trapping technique was applied to titania−CO_2 systems. Figure 6 presents EPR spectra recorded after 1 min of illumination of titania dispersions containing DMPO as a spin trap, all containing CO_2. The formation of DMPO−OH ($a_N = a_H = 1.48$ mT) and DMPO−CH_3 adducts ($a_N = 1.57$ mT, $a_H = 2.085$ mT) is observed both in the absence (Figure 6a) and in the presence (Figure 6b) of sodium carbonate. For these measurements, the pH of water was adjusted to 11 to match that of the sodium carbonate solution. The band edges change with pH according to the Nernst equation ($E_{CB} = -0.74$ V, and $E_{VB} = +2.46$ V at pH 11) and could affect charge transfer to adsorbed molecules, and thus the yield of products. A higher concentration of methyl radicals is formed in the presence of 0.5 M Na_2CO_3, as compared to the concentration of OH radicals, proving that

dx.doi.org/10.1021/ja108791u |*J. Am. Chem. Soc.* 2011, 133, 3964–3971

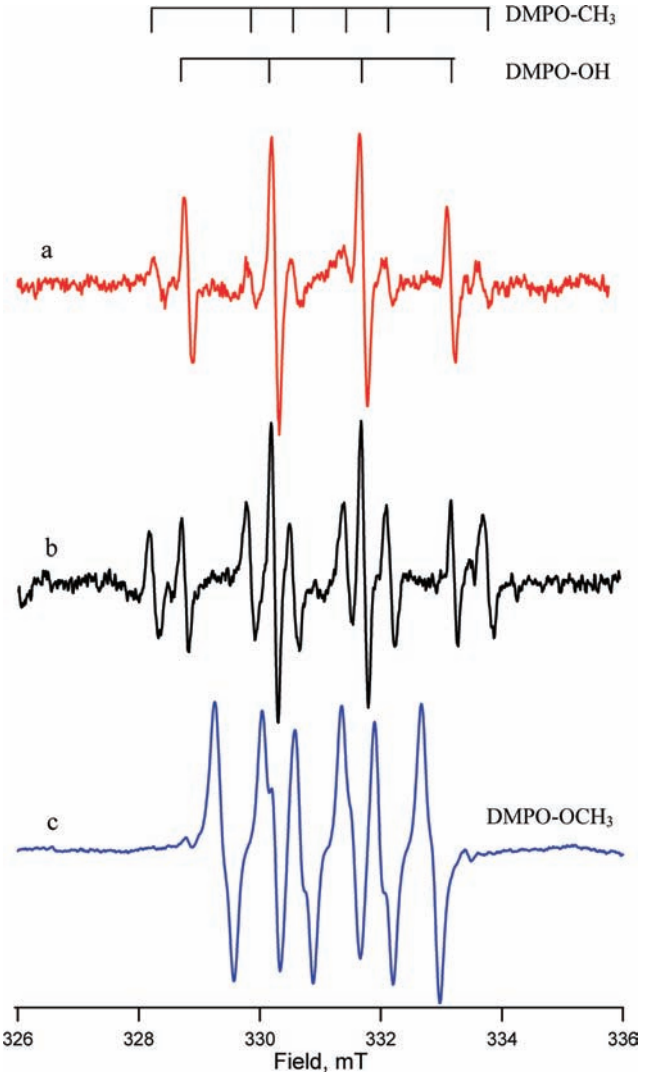

Figure 6. EPR spectra recorded at room temperature after 1 min of illumination of TiO_2-CO_2 and DMPO in (a) H_2O, pH 11, (b) 0.5 M aqueous Na_2CO_3, and (c) acetonitrile. Power, 33.2 mW; modulation amplitude, 0.1 mT; light source, 300-W Xe lamp. A capillary tube was filled with a solution of TiO_2 (20 mg/mL) and DMPO (60 mM) and placed in a vacuum, 4 mm diameter Suprasil tube. After degassing at 77 K, 6.2 mmol of CO_2 was introduced into the tube, and the whole setup was brought to room temperature.

carbonate ions act as electron donors, competing with water for photogenerated holes. Some of the OH radicals can be formed not only from direct reaction of valence band holes with water (eq 5) but also from reaction of H_2O_2 with surface-trapped electrons, $(Ti^{3+})_{surf}$, a Fenton-type reaction (eq 10). Due to the increased local concentration of OH radicals on the surface of TiO_2, the yield of H_2O_2 (formed from combination reaction of two OH radicals) is higher than in homogeneous systems.

$$H_2O_2 + (Ti^{3+})_{surf} \rightarrow OH + OH^- + (Ti^{4+})_{surf} \qquad (10)$$

When acetonitrile was used as a dispersant, allowing for illumination of partially hydrated TiO_2, the formation of an oxygen-centered methoxyl radical, $^{\bullet}OCH_3$, was detected (Figure 6c). The signal with hyperfine splitting constants a_N = 1.35 mT, a_H^{β} = 0.775 mT, and a_H^{γ} = 0.17 mT is attributed to a $DMPO-OCH_3$ adduct, in accordance with the literature values.[53] The generation of any type of hydrocarbon radical from "dry" TiO_2 P25 suggests that H atoms are formed from dissociated/submonolayer water rather than from bulk water. Bulk water leads to detachment of radicals from the surface, and the reaction of methoxyl radical with H_2O can lead to formation of methanol. Under our experimental conditions (the maximum concentration of DMPO used was 0.1 M), we did not observe $DMPO-H$ or $DMPO-CO_2^-$ adducts, which suggests a fast rate of hydrocarbon formation on the surface of TiO_2 at room temperature.

Scheme 2. Proposed Mechanism of Photocatalytic Transformation of CO_2 to Methoxyl Radical over TiO_2 in the Presence of Dissociated/Bound Water

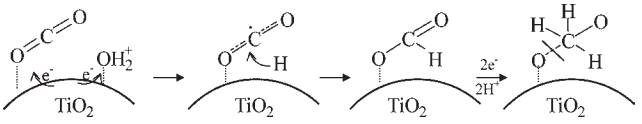

Initial Steps in CO_2 Reduction. The direct detection of H atoms and CH_3 radicals present simultaneously upon illumination of P25 with CO_2/H_2O (1:1 molar ratio) suggests competitive electron transfer to adsorbed/bound carbon dioxide and adsorbed/bound protons on the surface of TiO_2 (Scheme 2). The initial electron transfer is accompanied by breaking of the double O=C=O bond and attachment of a H atom, resulting in the formation of formate. Consecutive electron/proton transfer leads to formation of methoxyl radical.

The initial step in the proposed mechanism (competitive electron transfer) thus corresponds to two-electron, one-proton transfer, as shown in eq 11.

$$CO_2 + 2e^- + H^+ \rightarrow HCOO^- \qquad (11)$$

In order to estimate the energetics of the simultaneous two-electron process (eq 11) on the surface of TiO_2, theoretical modeling in the gas phase has been carried out. For this purpose we have considered the case where a reactant hydrogen is initially adsorbed on the two-fold bridging oxygen site and its electron is redistributed to the conduction band of TiO_2. It has been shown that the energies from localized and delocalized states of an extra electron on anatase (101) surface are nearly degenerate.[54] The extent of localization of the initial unpaired electron, although a topic of interest,[55] has little effect on the energies of surfaces.[56] Hence, the initial spatial distribution of the electron has little effect on the adsorption and reaction energies of the surfaces with an adsorbate in the case of charge transfer. The calculated reaction pathway is plotted in Figure 7.

We have chosen the sum of energies of an isolated CO_2 molecule and two protons ($2H^+$) adsorbed on the negatively charged ($2e^-$) anatase (101) surface as the energy reference (see Figure 7). As reported previously,[34] CO_2 prefers a linear vertical adsorption (labeled as A1 configuration) at the five-fold Ti site on the anatase (101) surface. It binds to the surface relatively weakly, with a binding energy of 0.21 eV, which is not affected by the presence of one adsorbed hydrogen in its vicinity $[CO_2(A1)\cdots H^+(a) + e^-]$. Co-adsorption of another proton nearby $[CO_2(A1)\cdots 2H^+(a) + 2e^-]$ results in a metastable state, which is unfavorable energetically by 0.26 eV relative to the proton farther away. In the presence of two H^+ adsorbed on the surface next to a CO_2 molecule and two extra electrons in the conduction band (representing photoexcited electrons), CO_2 can be activated and converted to formate, involving a concerted

dx.doi.org/10.1021/ja108791u |J. Am. Chem. Soc. 2011, 133, 3964–3971

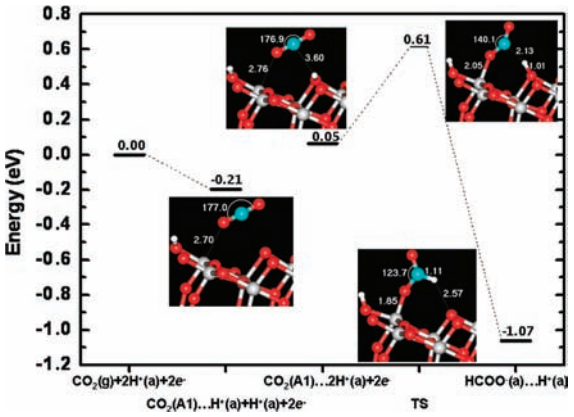

Figure 7. First-principles calculations of the reaction pathway from CO_2 and hydrogen to formate on the anatase (101) surface. Important bond lengths (Å) and angles (degrees) are marked in all geometries with atom colors showing Ti in gray, O in red, C in blue, and H in white. The species along the reaction pathway are labeled at the bottom, where "g" denotes gas phase and "a" denotes adsorbed species on the anatase (101) surface; A1 is a linear vertical adsorption configuration of CO_2 on the surface. The "+" sign indicates non-interacting species, while "..." indicates two species in proximity.

two-electron, one-proton transfer from the TiO_2 substrate. The transition state (TS) for this process in Figure 7 is represented by CO_2^- (one electron transferred already) strongly bound to the five-fold Ti site with a Ti−O distance of 2.05 Å and bent ($\angle$OCO ~140°) toward a proton adsorbed on the surface, forming a hydrogen bond 2.1 Å in length. The effective barrier for the formation of formate via a two-electron, one-proton process is calculated to be 0.82 eV, a value lower than the activation energy for one-electron transfer to CO_2 alone. The relatively high activation barrier of 0.82 eV would account for the relatively low efficiency determined experimentally at room temperature, together with the complex nature of the processes on the surface of TiO_2, considered here only for water and carbonates.

CONCLUSION

Water, both dissociated on the surface of TiO_2 and in subsequent molecular layers, has a three-fold role: (i) stabilization of charges (preventing electron−hole recombination), (ii) as an electron donor (reaction of water with photogenerated holes to give OH radicals), and (iii) as an electron acceptor (formation of H atoms in a reaction of photogenerated electrons with protons on the surface, $-OH_2^+$). Dissolved CO_2 in the form of carbonates/bicarbonates competes with water for photogenerated holes and thus can act as a hole scavenger. CO_3^- radicals are relatively strong one-electron oxidation agents. Finally, observation of such reaction intermediates as H atoms, $^{\bullet}OCH_3$ radicals, and $^{\bullet}CH_3$ radicals, and first-principles calculations, suggest a concerted two-electron, one-proton transfer to adsorbed carbon dioxide molecules, demonstrating the importance of hydrogen/water management on the photocatalyst surface.

ASSOCIATED CONTENT

Supporting Information. Determination of quantum yield for CH_4 formation; evolution of EPR spectra with time of illumination and CO_2 concentration, together with EPR spectra of reference samples (blank experiments), for both direct and spin-trap EPR measurements; electron density distribution from PBE calculations. This material is available free of charge via the Internet at http://pubs.acs.org.

AUTHOR INFORMATION

Corresponding Author
dimitrijevic@anl.gov

ACKNOWLEDGMENT

This work was performed under the auspices of the U.S. Department of Energy under Contract DE-AC02-06CH11357. Use of computational resources at Argonne National Laboratory Computing Resource Center is gratefully acknowledged.

REFERENCES

(1) Inoue, T.; Fujishima, S.; Konishi, S.; Honda, K. *Nature* **1979**, *277*, 637.
(2) Usubharatana, P.; McMartin, D.; Veawab, A.; Tontiwachwuthikul, P. *Ind. Eng. Chem. Res.* **2006**, *45*, 2558.
(3) Kitano, M.; Matsuoka, M.; Ueshima, M.; Anpo, M. *Appl. Catal., A: Gen.* **2007**, *325*, 1.
(4) Centi, G.; Perathoner, S. *Catal. Today* **2009**, *148*, 191.
(5) (a) Anpo, M.; Yamashita, H.; Ichihashi, Y.; Ehara, S. *J. Electroanal. Chem.* **1995**, *396*, 21. (b) Anpo, M.; Takeuchi, T. *J. Catal.* **2003**, *216*, 505. (c) Anpo, M.; Thomas, J. M. *Chem. Commun.* **2006**, 3273.
(6) Chen, L.; Graham, M. E.; Li, G.; Gentner, D. R.; Dimitrijevic, N. M.; Gray, K. A. *Thin Solid Films* **2009**, *517*, 5641.
(7) Nguyen, T. V.; Wu, J. C. S.; Chiou, C. H. *Catal. Commun.* **2008**, *9*, 2073.
(8) Ozcan, O.; Yukruk, F.; Akkaya, E. U.; Uner, D. *Top. Catal.* **2007**, *44*, 523.
(9) Woolerton, T. W.; Sheard, S.; Reisner, E.; Pirece, E.; Ragsdale, S. W.; Armstrong, F. A. *J. Am. Chem. Soc.* **2010**, *132*, 2132.
(10) Tseng, I. H.; Chang, W. C.; Wu, J. C. S. *Appl. Catal., B* **2002**, *37*, 37.
(11) Wu, J. C. S. *Catal. Surv. Asia* **2009**, *13*, 30.
(12) Wang, C.; Thompson, R. L.; Baltrus, J.; Matranga, C. *J. Phys. Chem. Lett.* **2010**, *1*, 48.
(13) Kaneco, S.; Shimizu, Y.; Ohta, K.; Mizuno, T. *J. Photochem. Photobiol. A* **1998**, *115*, 223.
(14) Tseng, I. H.; Chang, W. C.; Wu, J. C. S. *Appl. Catal. B: Environ.* **2002**, *37*, 37.
(15) Belapurkar, A. D.; Kishore, K. *J. Photochem. Photobiol. A* **2004**, *163*, 503.
(16) Dey, G. R.; Pushpa, K. K. *Res. Chem. Intermed.* **2007**, *33*, 631.
(17) (a) Duonghong, D.; Ramsden, J. M.; Gratzel, M. *J. Am. Chem. Soc.* **1982**, *104*, 2977. (b) Dimitrijevic, N. M.; Savic, D.; Micic, O. I.; Nozik, A. J. *J. Phys. Chem.* **1984**, *88*, 4278.
(18) Centi, G.; Perathoner, S.; Wine, G.; Gangeria, M. *Green Chem.* **2007**, *9*, 671 and references cited therein.
(19) Lunsford, J. H.; Jayne, J. P. *J. Phys. Chem.* **1965**, *69*, 2182.
(20) (a) Tanaka, T.; Kohno, Y.; S. Yoshida, S. *Res. Chem. Intermed.* **2000**, *26*, 93. (b) Teramura, K.; Tanaka, T.; Ishikawa, H.; Kohno, Y.; Funabiki, T. *J. Phys. Chem. B* **2004**, *108*, 346.
(21) (a) Chiesa, M.; Giamello, E. *Chem.—Eur. J.* **2007**, *13*, 1261. (b) Preda, G.; Pacchioni, G.; Chiesa, M.; Giamello, E. *J. Phys. Chem. C* **2008**, *112*, 19568.
(22) J. Rasko, J.; Solymosi, F. *J. Phys. Chem.* **1994**, *98*, 7147.
(23) Yoneyama, H. *Catal. Today* **1997**, *39*, 169.
(24) Hemminger, J. C.; Carr, R.; Somorjai, G. A. *Chem. Phys. Lett.* **1978**, *57*, 100.
(25) Green, J.; Carter, E.; Murphy, D. M. *Chem. Phys. Lett.* **2009**, *477*, 340.
(26) Henderson, M A. *Langmuir* **1996**, *12*, 5093.

(27) Ketteler, G.; Yamamoto, S.; Bluhm, H.; Andersson, K.; Starr, D. E.; Ogletree, D. F.; Ogasawara, H.; Nilsson, A.; Salmeron, M. *J. Phys. Chem. C* **2007**, *111*, 8278.
(28) He, Y.; Tilocca, A.; Dulub, O.; Selloni, A.; Diebold, U. *Nat. Mater.* **2009**, *8*, 858.
(29) Levchenko, A. A.; Li, G.; Boerio-Goates, J.; Woodfield, B. F.; Navrotsky, A. *Chem. Mater.* **2006**, *18*, 6324.
(30) Vijayan, B.; Dimitrijevic, N. M.; Rajh, T.; Gray, K. A. *J. Phys. Chem. C* **2010**, *114*, 12994.
(31) Perdew, J. P.; Burke, K.; Ernzerhof, M. *Phys. Rev. Lett.* **1996**, *77*, 3865.
(32) Kresse, G.; Furthmuller, J. *Phys. Rev. B* **1996**, *54*, 11169.
(33) Lazzeri, M.; Vittadini, A.; Selloni, A. *Phys. Rev. B* **2001**, *63*, 155409.
(34) He, H.; Zapol, P.; Curtiss, L. *J. Phys. Chem. C* **2010**, *114*, 21474.
(35) Sanville, E.; Kenny, S. D.; Smith, R.; Henkelman, G. *J. Comput. Chem.* **2007**, *28*, 899.
(36) Henkelman, G.; Jonsson, H. *J. Chem. Phys.* **2000**, *113*, 9978.
(37) Parmon, V.; Emeline, A. V.; Serpone, N. *Int. J. Photoenergy* **2002**, *4*, 91.
(38) Hurum, D. C.; Agrios, A. G.; Gray, K. A.; Rajh, T.; Thurnauer, M. C. *J. Phys. Chem. B* **2003**, *107*, 4545.
(39) (a) Berger, T.; Sterrer, M.; Diwald, O.; Knozinger, E.; Panayotov, D.; Thompson, T. L.; Yates, J. T., Jr. *J. Phys. Chem. B* **2005**, *109*, 6061. (b) Berger, T.; Sterrer, M.; Diwald, O.; Knozinger, E. *Chem. Phys. Chem.* **2005**, *6*, 2104.
(40) Enright, B.; Fitzmaurice, D. *J. Phys. Chem.* **1996**, *100*, 1027.
(41) (a) Kumar, C. P.; Gopal, N. O.; Wang, T.-C.; Wong, M.-S.; Ke, S.-C. *J. Phys. Chem. B* **2006**, *110*, 5223. (b) Ke, S.-C.; Wang, T.-C.; Wong, M.-S.; Gopal, N. O. *J. Phys. Chem. B* **2006**, *110*, 11628.
(42) See for example: Rajh, T.; Makarova, O. V.; Thurnauer, M. C.; Cropek, D. In *Synthesis, Functionalization and Surface Treatment of Nanoparticles*; Baraton, M.-I., Ed.; American Science Publishers: Valencia, CA, 2003; pp 147−171.
(43) Dimitrijevic, N. M.; Poluektov, O. G.; Saponjic, Z. V.; Rajh, T. *J. Phys. Chem. B* **2006**, *110*, 25392.
(44) Bielski, B.; Gebicki, J. M. *Atlas of Electron Spin Resonance Spectra*; Academic Press: New York/London, 1967.
(45) (a) Florin, R. E.; Brown, H. W.; Wall, L. A. *J. Phys. Chem.* **1962**, *66*, 2672. (b) Fessenden, R. W.; Schuler, R. H. *J. Chem. Phys.* **1963**, *39*, 2147.
(46) (a) Rodriguez, R.; Blesa, M. A.; Regazzoni, A. E. *J. Colloid Interface Sci.* **1996**, *177*, 122. (b) Erdem, B.; Hunsicker, R. A.; Simmons, G. W.; Sudol, E. D.; Dimonie, V. L .; El-Aasser, M. S. *Langmuir* **2001**, *17*, 2664.
(47) Dimitrijevic, N. M.; Saponjic, Z. V.; Rabatic, B. M.; Poluektov, O. G.; Rajh, T. *J. Phys. Chem. C* **2007**, *111*, 14597.
(48) See for example: (a) Hoffmann, M. R.; Martin, S. T.; Choi, W.; Bahnemann, D. W. *Chem. Rev.* **1995**, *95*, 69. (b) Mills, A.; Le Hunte, S. *J. Photochem. Photobiol. A Chem.* **1997**, *108*, 1.
(49) Jaeger, C. D.; Bard, A. J. *J. Phys. Chem.* **1979**, *83*, 3146.
(50) Giamello, E.; Calosso, L.; Fubini, B.; Geobaldo, F. *J. Phys. Chem.* **1993**, *97*, 5735.
(51) (a) Chantry, G. W.; Horsfield, A.; Morton, J. R.; Whiffen, D. H. *Mol. Phys.* **1962**, *5*, 589. (b) Serway, R. A.; Marshal, S. A. *J. Chem. Phys.* **1967**, *47*, 868. (c) Koksal, F.; Koseoglu, R. *Radiat. Phys. Chem.* **2000**, *57*, 59.
(52) Goren, Z.; Willner, I.; Nelson, A. J.; Frank, A. J. *J. Phys. Chem.* **1990**, *94*, 3784.
(53) (a) Li, A. S. W.; Cummings, K. B.; Roethling, H. P.; Buettner, G. R.; Chignell, C. F. *J. Magn. Reson.* **1988**, *79*, 140. (b) Izakovic, M.; Sima, J.; Brezova, V. *J. Photochem. Photobiol. A* **2004**, *167*, 81.
(54) Di Valentin, C.; Pacchioni, G.; Selloni, A. *J. Phys. Chem. C* **2009**, *113*, 20543.
(55) Minato, T.; Sainoo, Y.; Kim, Y.; Kato, H. S.; Aika, K.; Kawai, M.; Zhao, J.; Petek, H.; Huang, T.; He, W.; Wang, B.; Wang, Z.; Zhao, Y.; Yang, J.; Hou, G *J. Chem. Phys.* **2009**, *130*, 124502.
(56) Deskins, N. A.; Rousseau, R.; Dupuis, M. *J. Phys. Chem. C* **2010**, *114*, 5891.